

The plasma filling factor of coronal bright points (Research Note)

II. Combined EIS and TRACE results

K. P. Dere

Department of Computational and Data Sciences, George Mason University, 4400 University Dr., Fairfax VA, 22030, USA
e-mail: kdere@gmu.edu

Received 11 November 2008 / Accepted 28 January 2009

ABSTRACT

Aims. In a previous paper, the volumetric plasma filling factor of coronal bright points was determined from spectra obtained with the Extreme ultraviolet Imaging Spectrometer (EIS). The analysis of these data showed that the median plasma filling factor was 0.015. One interpretation of this result was that the small filling factor was consistent with a single coronal loop with a width of 1–2", somewhat below the apparent width. In this paper, higher spatial resolution observations with the Transition Region and Corona Explorer (TRACE) are used to test this interpretation.

Methods. Rastered spectra of regions of the quiet Sun were recorded by the EIS during operations with the Hinode satellite. Many of these regions were simultaneously observed with TRACE. Calibrated intensities of Fe XII lines were obtained and images of the quiet corona were constructed from the EIS measurements. Emission measures were determined from the EIS spectra and geometrical widths of coronal bright points were obtained from the TRACE images. Electron densities were determined from density-sensitive line ratios measured with EIS. A comparison of the emission measure and bright point widths with the electron densities yielded the plasma filling factor.

Results. The median electron density of coronal bright points is $3 \times 10^9 \text{ cm}^{-3}$ at a temperature of $1.6 \times 10^6 \text{ K}$. The volumetric plasma filling factor of coronal bright points was found to vary from 3×10^{-3} to 0.3 with a median value of 0.04.

Conclusions. The current set of EIS and TRACE coronal bright-point observations indicate the median value of their plasma filling factor is 0.04. This can be interpreted as evidence of a considerable subresolution structure in coronal bright points or as the result of a single completely filled plasma loop with widths on the order of 0.2–1.5" that has not been spatially resolved in these measurements.

Key words. Sun: corona

1. Introduction

In a previous paper, Dere (2008, hereafter referred to as Paper I), rastered spectra obtained with the Extreme ultraviolet Imaging Spectrometer (EIS) were analyzed to determine the plasma filling factor of coronal bright points. This study was motivated by Parker's suggestion that coronal heating occurs through the dissipation of magnetic discontinuities on very fine scales (Parker 1988). There is currently considerable interest in trying to explain the structure and energetics of coronal loops with ensembles of subresolution, transient threads of emitting plasma (Cargill & Klimchuk 1997).

In Paper I, measurements of 62 coronal bright point were presented and analyzed. Some of these measurements were of the same bright point but at different times. Measurements include the loop widths, peak intensities, and electron densities based on Fe XII line profiles. The median electron density of coronal bright points in this set of measurements was $4 \times 10^9 \text{ cm}^{-3}$ and the median plasma filling factor was 0.015. Electron densities derived from density-sensitive line-ratios of Fe XIII for a subset of these bright points, suggested that the electron density could be a factor of 2 lower. This would result in a filling factor a factor of 4 larger, or, a value of 0.06. If the coronal bright points were interpreted as due to single subresolution loops, then these subresolution loops would have a median width of 0.9", or 1.8" if the Fe XIII densities were used.

These results indicated that coronal bright points were made up of structures below the limit of the EIS spatial resolution. These subresolution structure could consist of a single filled loop, multiple filled loops or more diffuse structures. Based on these observations, it is not possible to discern between these models or some other model.

In that paper, it was also suggested that the EIS observations could be compromised by the jitter in the Hinode spacecraft point that directly controls the EIS pointing. Typical values of the jitter seem to be on the order of 3–5", although it is not clear exactly what value would be appropriate for the data set analyzed in Paper I. In light of this, it was suggested that it would be useful to analyze Transition Region and Corona Explorer (TRACE) observations which nominally have a spatial resolution a factor of 2 better than EIS and closer to the inferred 0.9 to 1.8" widths of the hypothetical subresolution loops.

2. Instrumentation, observations and data reduction

The instrumentation and observations were described in Paper I. In addition to those observations, a similar program was carried out on June 16 when 4 series of 3 consecutive, contiguous 55" rasters were performed to cover a region about $165" \times 512"$. These rasters were not analyzed in Paper I but are used here. A

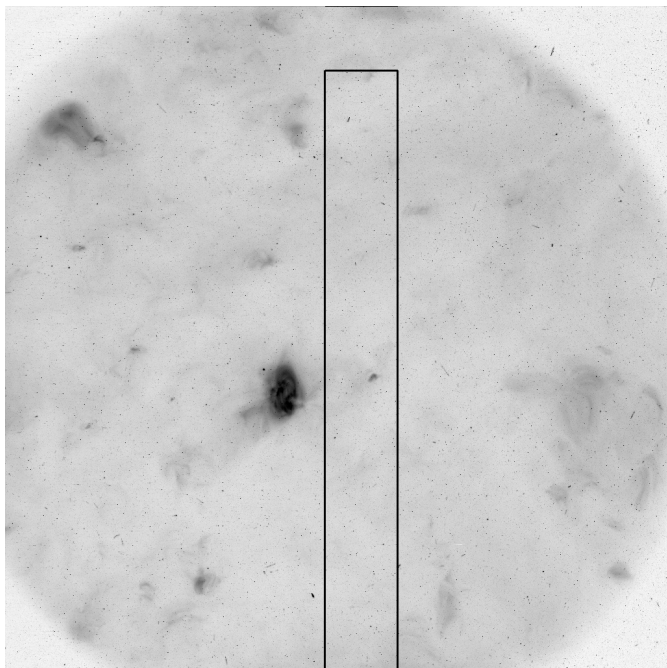


Fig. 1. TRACE image in Fe XII $\lambda 195$, obtained on 2007 June 17 at 0937 UT, with an outline of the area of the EIS raster, obtained on 2007 June 17 from 0920 to about 1020 UT. The area of the image is $512''$ by $512''$.

set of labels were also applied to the bright points as discussed in Paper I and they are used here as well.

Included in the EIS data processing are procedures to remove the effect of “hot” and “warm” pixels. This is accomplished by identifying these pixels and assigning a weight of zero in the Gaussian profile fitting. However, it is not possible to correctly identify all of these pixels. The “warm” pixels tend to come and go on time scales ranging from a few hours to weeks. Their visible effect is to leave streaks or lines along the rastered spectral intensity and density images. The derivation of the quantities used in this analysis, intensity, density and width, is a highly interactive procedure.

Roughly simultaneous observations were made with TRACE during the period of June 16–18. The TRACE 195 Å bandpass images were used to correspond to the Fe XII spectra analyzed here. An example of the area covered by an EIS raster is outlined in the TRACE image shown in Fig. 1. In order to measure the low intensity coronal bright points with TRACE, it was necessary to use exposure times of 262 s, the longest in the TRACE sequence. Of the 32 EIS rasters obtained during this period, 20 had nearly simultaneous TRACE observations. The TRACE instrument has been described in detail by Handy et al. (1999).

3. Electron densities and filling factors in coronal bright points

The measurements needed to determine the plasma filling factor of coronal bright points are the central intensity, the full width at half maximum (FWHM), and the electron density. These measurements were made in the same manner as in Paper I, with the exception that the loop widths were determined from the FWHM of the profile of the TRACE intensities across the bright point. The electron densities were determined from density-sensitive lines of Fe XII by means of the atomic model provided by the CHIANTI database (Dere et al. 1997; Landi et al. 2006). Several

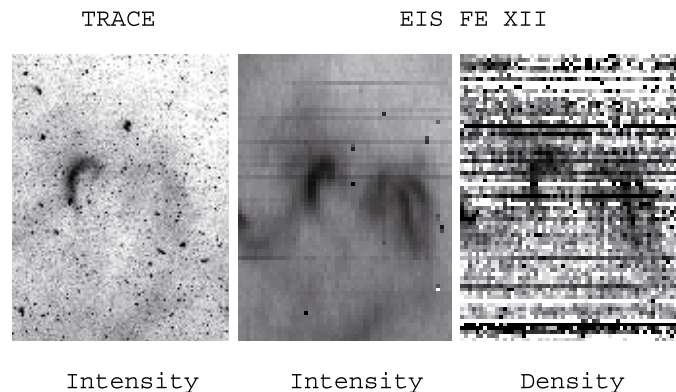


Fig. 2. TRACE Fe XII $\lambda 195$ image of coronal bright point 13 obtained on 2007 June 16 at 01:22 UT and coaligned EIS Fe XII intensity and density images obtained in a raster starting at 00:31 UT. The area of the images is $55''$ (east-west) by $74''$ (north-south). The densities are logarithmically scaled from $10^{8.3} \text{ cm}^{-3}$ (white) to $10^{9.3} \text{ cm}^{-3}$ (black).

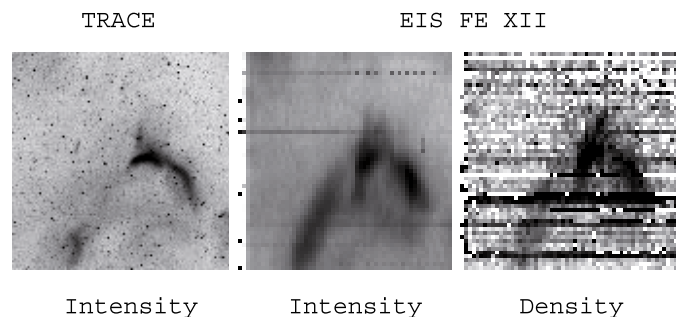


Fig. 3. TRACE Fe XII $\lambda 195$ image of coronal bright point 35 and 36 obtained on 2007 June 16 at 2037 UT and coaligned EIS Fe XII intensity and density images obtained in a raster starting at 2029 UT. The area of the images is $55''$ (east-west) by $56''$ (north-south). The densities are logarithmically scaled from $10^{8.3} \text{ cm}^{-3}$ (white) to $10^{9.5} \text{ cm}^{-3}$ (black).

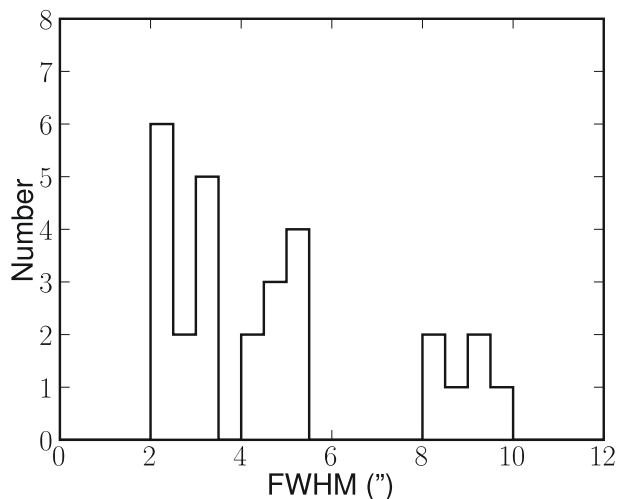


Fig. 4. Histogram of TRACE FWHM measurements.

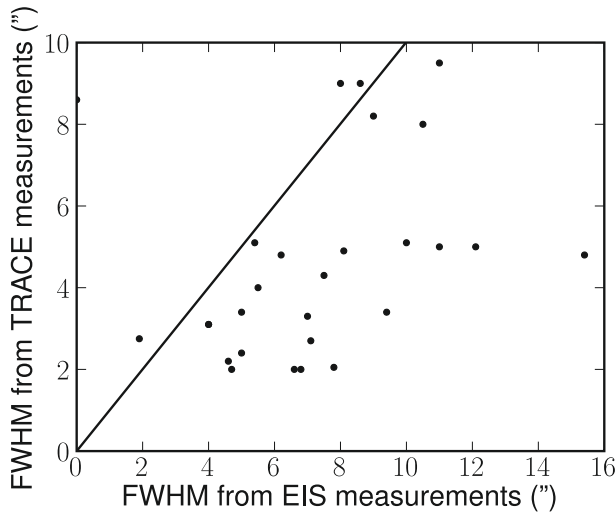
examples of coaligned TRACE and EIS coronal bright point observations are shown in Figs. 2 and 3. The E-W streaks are caused by the unsuccessful identification of “hot” and “warm” pixels in the data processing, as discussed above. The measurements for the observations obtained on June 16 are shown in Table 1 and for those obtained on June 17–18 in Table 2. The median electron density for all of these measurements is $3 \times 10^9 \text{ cm}^{-3}$ and is comparable to the value for the

Table 1. Coronal bright point intensities, densities, widths, filling factors, and subresolution widths for observations on 2007 June 16.

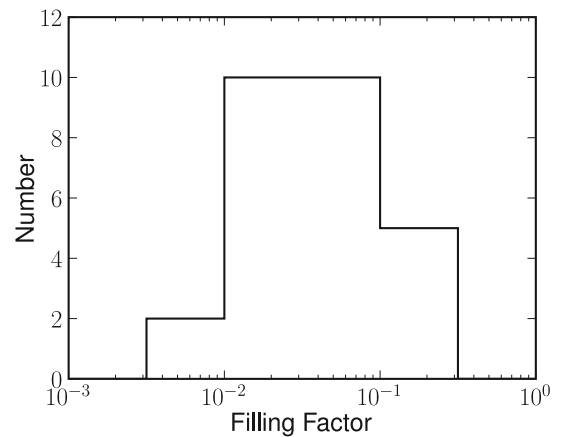
Label	EIS UT	TRACE UT	Intensity $\text{erg cm}^{-2} \text{s}^{-1} \text{sr}^{-1}$	Log density (cm^{-3})	Width ($''$)	Filling factor	Corrected width ($''$)	Length ($''$)
A	11:59	12:44	4.84e+02	9.59	2.0	2.2e-01	0.9	19.4
11	05:25	06:16	8.61e+01	9.67	4.9	1.1e-02	0.5	
11	11:59	12:44	1.87e+02	9.77	2.0	3.7e-02	0.4	6.0
13	00:31	01:22	1.26e+02	9.3	3.1	1.4e-01	1.2	13.5
13	02:11	02:59	1.23e+02	9.23	4.8	1.2e-01	1.7	
14	00:31	01:22	9.69e+01	9.39	4.0	5.6e-02	0.9	9.3
25	02:11	02:59	9.69e+01	9.46	2.0	8.1e-02	0.6	
25	17:14		8.25e+02	10.3	3.4	8.5e-03	0.3	7.5
26	02:11	02:59	1.04e+02	9.4	4.3	5.4e-02	1.0	
26	13:38	14:12	3.34e+02	9.76	3.4	4.1e-02	0.7	
27	03:47	04:36	4.52e+02	9.56	5.0	9.6e-02	1.5	
28	03:47	04:36	1.18e+02	9.45	8.0	2.6e-02	1.3	10.6
31	11:59	12:44	1.08e+02	9.62	2.8	3.2e-02	0.5	2.5
32	11:59	12:44	2.87e+02	9.57	2.7	1.1e-01	0.9	5.9
35	17:14		1.33e+02	9.81	2.0	2.2e-02	0.3	7.2
35	20:29	20:37	2.22e+02	10.04	2.4	1.1e-02	0.2	6.4
36	20:29	20:37	2.62e+02	9.53	3.1	1.0e-01	1.0	8.9

Table 2. Coronal bright point intensities, densities, widths, filling factors, and subresolution widths for observations on 2007 June 17–18.

Label	Raster	TRACE UT	Intensity $\text{erg cm}^{-2} \text{s}^{-1} \text{sr}^{-1}$	Log density (cm^{-3})	Width ($''$)	Filling factor	Corrected width ($''$)	Length ($''$)
B	4	09:37	2.65e+02	10.21	3.3	4.3e-03	0.2	6.4
F	15	06:20	1.40e+03	9.97	5.0	4.5e-02	1.1	9.3
F	17	14:12	7.89e+02	9.87	8.2	2.5e-02	1.3	20.2
G	10	23:58	1.74e+02	9.65	9.5	1.3e-02	1.1	19.0
G	15	06:20	2.73e+02	9.65	4.8	4.0e-02	1.0	18.5
H	10a	23:58	1.84e+02	9.5	9.0	2.9e-02	1.5	23.5
H	10b	23:58	1.97e+02	9.5	9.0	3.1e-02	1.6	18.0
H	15a	06:20	1.11e+02	9.3	5.1	7.7e-02	1.4	19.3
H	15b	06:20	1.29e+02	9.3	5.1	8.9e-02	1.5	19.3
K	17	14:12	8.25e+01	9.73	2.2	1.8e-02	0.3	2.5

**Fig. 5.** Comparison of EIS and TRACE FWHM measurements.

electron densities reported in Paper I. As discussed in Dere et al. (2007), the root-mean-square error in the determination of electron densities in the quiet Sun, including bright points, is a factor of 1.6. A histogram of the TRACE FWHM measurements is shown in Fig. 4 and the median value is 3.5''. Figure 5 shows a comparison of TRACE and EIS FWHM measurements. The solid line in the figure shows where a 1 to 1 relationship would

**Fig. 6.** Histogram of coronal bright point filling factors.

lie. Generally the TRACE measurements reveal spatial scales less than the EIS observations.

The distribution of plasma filling factors, derived in the same manner as in Paper I but with the TRACE FWHM measurements, is shown in Fig. 6. The median value is 0.04, about a factor of 2.7 greater than the filling factor of 0.015 derived solely from EIS measurements in Paper I. Also in the same manner as in Paper I, the width of a single subresolution coronal loop that is consistent with the observed electron density and intensity is

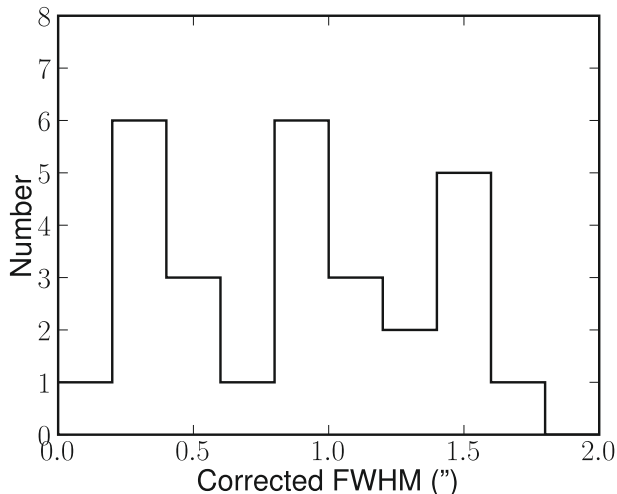


Fig. 7. Histogram of the widths of single subresolution loops consistent with the observed intensities and densities.

provided in Tables 1, 2 and their distribution is shown in Fig. 7. The median value is $0.95''$, and if the electron densities were a factor of 2 lower, as suggested from Fe XIII measurements, the median value would be $1.9''$. These are essentially identical to the values derived in Paper I.

4. Discussion

The principle goal in essentially repeating these measurements was to use the better spatial resolution of TRACE to completely resolve the coronal bright points which were predicted to have widths of $1''$ to $2''$, assuming they consisted of a single, fully filled coronal loop. As seen in Fig. 5, the coronal bright point widths determined from the TRACE images are almost always less than those determined from EIS images. The minimum EIS width is about $4''$ and the minimum TRACE width is about $2''$, roughly consistent with the 2:1 spatial resolution.

Aschwanden et al. (2000) have measured the physical properties of 41 coronal loops with TRACE data. They find loop widths ranging from 1.5 Mm ($2.1''$) to 7.5 Mm ($10.3''$) and note that the shortest loops have an average diameter of 2.5 Mm ($3.4''$). For their loops with lengths comparable to those of the coronal bright points analyzed here, the measurements listed in their Table 3 indicate an average width of 1.9 Mm ($2.7''$), a value that is compatible with the lowest values of our TRACE loop width measurements.

For the largest structures, the measurements TRACE and EIS are about the same. If it is assumed that the EIS widths are given by the quadrature sum of the actual loop width and the total EIS resolution in the area where the TRACE widths are about $2''$ to $5''$, then the total EIS resolution is about $4''$ to $8''$. The total EIS resolution would then consist of the quadrature sum of actual spatial resolution of the EIS instrument and the Hinode spacecraft jitter.

The TRACE measurements have yielded generally lower values for the loop width and consequently higher values for the filling factors. Nevertheless, the plasma filling factor remains small with a median value of 0.04 to perhaps 0.16, indicating the existence of spatial scales below those measurable with TRACE. The minimum loop widths determined by the present measurements and those of Aschwanden et al. (2000) are both at the level of about $2''$. This suggests that it is unlikely that further measurements with TRACE will be able to clarify the exact nature of the subresolution structure: do they consist of single filled plasma loops, multiple filled plasma loops or more diffuse structures?

If these bright points do consist of single filamentary structures with widths on the order of $1''$, then instrumentation with a spatial resolution about 3 times higher than possible with TRACE is needed to make definitive measurements to resolve this question in the future.

5. Conclusions

In Paper I, we measured the plasma filling factor of coronal bright points with rastered EIS spectra. A median plasma filling factor of 0.015 was determined. This was clear evidence for considerable subresolution structure. One possibility, among several, was that each bright point consisted of a single subresolution filamentary structure that would have a widths of about $1''$ to $2''$. The goal of this paper was to use the higher resolution TRACE observations to provide more definitive measurement of the loop widths and, hopefully, a better estimate of the filling factor and the widths of any single filamentary structures that are consistent with the observations.

The TRACE measurements are consistent with a plasma filling factor considerably below unity and suggest that any subresolution filaments that make up the bright points must have widths of $0.2''$ to $1.5''$ or less. The question of the nature of the subresolution structure of coronal bright points remains open.

Acknowledgements. Hinode is a Japanese mission developed and launched by ISAS/JAXA, with NAOJ as domestic partner and NASA and STFC (UK) as international partners. It is operated by these agencies in co-operation with ESA and NSC (Norway). We are grateful for the use of TRACE data. This research has made use of NASA's Astrophysics Data System.

References

- Aschwanden, M. J., Nightingale, R. W., & Alexander, D. 2000, ApJ, 541, 1059
- Cargill, P. J., & Klimchuk, J. A. 1997, ApJ, 478, 799
- Dere, K. P. 2008, A&A, 491, 561
- Dere, K. P., Landi, E., Mason, H. E., Monsignori Fossi, B. C., & Young, P. R. 1997, A&AS, 125, 149
- Dere, K. P., Doschek, G. A., Mariska, J. T., et al. 2007, PASJ, 59, 721
- Handy, B. N., Acton, L. W., Kankelborg, C. C., et al. 1999, Sol. Phys., 187, 229
- Landi, E., Del Zanna, G., Young, P. R., et al. 2006, ApJS, 162, 261
- Parker, E. N. 1988, ApJ, 330, 474